

Generalized Graph Convolutional Networks for Skeleton-based Action Recognition

Xiang Gao¹, Wei Hu¹, Jiaxiang Tang¹, Pan Pan², Jiaying Liu¹, Zongming Guo¹

¹Institute of Computer Science and Technology, Peking University, China

²Alibaba Group, China

¹{gyshgx868, forhuwei, hawkey1999, liujiaying, guozongming}@pku.edu.cn

²panpan.pp@alibaba-inc.com

Abstract—With the prevalence of accessible depth sensors, dynamic human body skeletons have attracted much attention as a robust modality for action recognition. Previous methods model skeletons based on RNN or CNN, which has limited expressive power for irregular joints. In this paper, we represent skeletons naturally on graphs and propose a generalized graph convolutional neural networks (GGCN) for skeleton-based action recognition, aiming to capture space-time variation via spectral graph theory. In particular, we construct a generalized graph over consecutive frames, where each joint is not only connected to its neighboring joints in the same frame strongly or weakly, but also linked with relevant joints in the previous and subsequent frames. The generalized graphs are then fed into GGCN along with the coordinate matrix of the skeleton sequence for feature learning, where we deploy high-order and fast Chebyshev approximation of spectral graph convolution in the network. Experiments show that we achieve the state-of-the-art performance on the widely used NTU RGB+D, UT-Kinect and SYSU 3D datasets.

I. INTRODUCTION

Action recognition is an active research direction in computer vision, with widespread applications in video surveillance, human computer interaction, robot vision, autonomous driving and so on. Among the multiple modalities [1], [2], [3], [4], [5] that are able to recognize human action, such as appearance, depth and body skeletons [6], [7], the skeleton-based sequences are springing up in recent years, due to the prevalence of affordable depth sensors (e.g., Kinect) and effective pose estimation algorithms [8]. Skeletons convey compact 3D position information of the major body joints, which are robust to variations of viewpoints, body scales and motion speeds [9]. Hence, skeleton-based action recognition has attracted more and more attention [10], [11], [12], [13], [14], [15], [16].

Different from modalities defined on regular grids such as images or videos, dynamic human skeletons are non-Euclidean geometric data, which consists of a series of human joint coordinates. This poses challenges in capturing both the intra-frame features and temporal dependencies. Recent methods learn these features via deep models like recurrent neural networks (RNN) [6], [7], [17], [18], [19], [20], [21], [22], [23] and convolutional neural networks (CNN) [21], [24], [25], [26], [27]. Nevertheless, the topology in skeletons is not fully exploited in the grid-shaped representation of RNN and CNN.

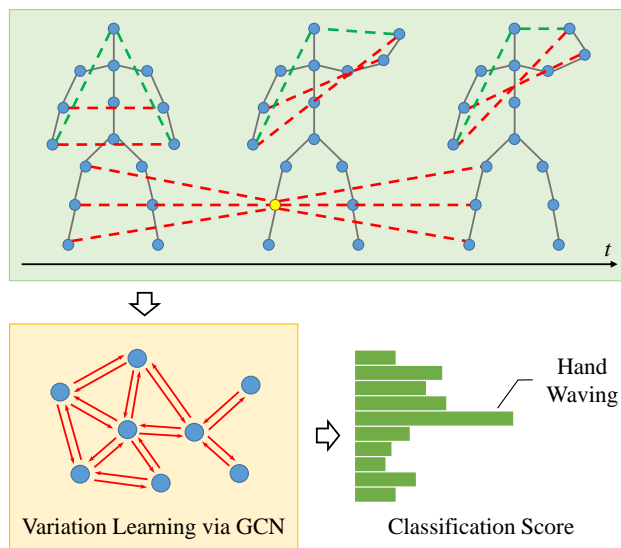


Fig. 1. **The pipeline of the proposed Generalized GCN for skeleton-based action recognition.** Given a sequence of human body joints, we first construct a *generalized graph* over each frame, its previous frame and the subsequent one via strong and physical edges (black solid lines), strong and non-physical edges (red dashed lines) and weak edges (green dashed ones) for *variation modeling*. We then feed the generalized graphs into a graph convolutional network (GCN) along with the 3D coordinates of joints for variation learning, which leads to classification scores.

A natural way to represent skeletons is graph, where each joint is treated as a vertex in the graph, and the relationship among the joints is interpreted by edges with weights. As unordered graphs cannot be fed into RNN or CNN directly, graph convolutional neural networks have been proposed to deal with data defined on irregular graphs for a variety of applications [28], [29], [30], [31]. Yan et al. [32] and Li et al. [33] are the first to propose graph-based skeleton representation, which is then fed into graph convolutional neural networks (GCNN) to automatically learn the spatial and temporal patterns from data. Tang et al. [34] propose a deep progressive reinforcement learning (DPRL) method to select the most informative frames of the input sequences and leverage GCNN to learn the dependency among joints. However, the graph constructions in these methods have certain limitations: graphs in [32] are

restricted by small partitions, graphs in [33] only model joints bridged by a bone, while there is no explicit temporal graph in [34]. Further, theoretical analysis of the graph construction has not been provided.

In order to further improve the graph construction of skeleton data for stronger expressive power, we propose Generalized Graph Convolutional Networks, where *generalized spatial-temporal graphs* are constructed over consecutive frames to model both spatial correlations and causal temporal dependencies, providing an alternate view of the action sequence. This is based on our *modeling of the variation* of skeletons via spectral graph theory [35], where the Laplacian matrix¹ of the generalized spatial-temporal graph extracts the variation of the coordinates of joints via Chebyshev approximation [31] of graph convolution. The captured variation is then leveraged to learn action features for final classification. As graph construction is crucial to the variation modeling, we carefully design the generalized graph according to the correlation among joints. Each joint in the target frame is not only connected to its neighboring joints in the same frame, but also linked with relevant joints in the other two frames, which enables learning the variation of the position of joints both spatially and temporally. Also, we model both strong and weak correlations among joints in space and time with graph edges of different weights. Strong correlations reflect physical connections or strong relationship among non-physical joints, while weak correlations represent potential relationship among joints that are not physically connected. This strengthens learning actions which are accomplished by joints that are not bridged by bones, such as “drink water” with the interaction between one hand and the head. Based on the constructed generalized graphs, we then deploy spectral graph convolutions with fast Chebyshev approximation for feature learning, which leads to final classification scores.

In summary, our contributions include the following aspects:

- We theoretically model the variation in a skeleton sequence on graphs based on spectral graph theory, which leads to the proposed generalized graph representation for capturing the variation.
- We apply GCNN to the input skeleton sequences and the constructed graph. When integrated with the generalized graph, the network is able to capture the variation of joint coordinates, thus leading to effective action feature learning.
- We achieve the state-of-the-art performance on the widely used NTU RGB+D, UT-Kinect and SYSU 3D datasets, and validate the effectiveness of the proposed generalized graph construction.

¹This matrix is an algebraic representation of the topology/connectivity of the corresponding graph in spectral graph theory, which will be defined in Sec. III

II. RELATED WORK

A. Skeleton-based Action Recognition

Previous skeleton-based action recognition methods can be divided into 2 classes [32]: hand-crafted feature based methods and deep learning methods.

Hand-crafted feature based methods. Hand-crafted features include covariance matrix for skeleton joint locations over time as a discriminative descriptor [36], modeling human actions as curves in the Lie group [14], and Spatio-Temporal Naive-Bayes Nearest-Neighbor [16], etc. However, these methods either lose information of interactions between specific sets of body parts or depend on complicated hand-crafted features.

Deep learning methods. Recent methods learn features via deep learning due to the notable performance, including RNN [6], [7], [17], [18], [19], [20], [21], [22], [23] and CNN [21], [24], [25], [26], [27]. However, these methods typically lose structural information when converting the raw skeleton data into the grid-shaped input of the neural networks. A natural way to address this issue is to represent skeleton data on graphs. Yan et al. [32] and Li et al. [33] are the first to employ graph convolutional neural networks (GCNN) to automatically learn both the spatial and temporal patterns from data. Specifically, Yan et al. [32] construct graph convolution operations on partitions, which however may not capture the relationship among joints in different partitions due to the small receptive field. Li et al. [33] design multi-scale convolutional filters, and simultaneously perform local convolutional filtering on temporal motions and spatial structures. For each frame, an undirected graph is constructed, where only joints bridged by a bone are connected, whereas there is no explicit temporal connectivity. Tang et al. [34] propose a deep progressive reinforcement learning (DPRL) method to select the most informative frames of the input sequences and apply GCNN to learn the spatial dependency between the joints. Edges in the constructed graph reflect both intrinsic dependencies (i.e., physical connection) and extrinsic dependencies (i.e., physical disconnection) by different weights. Nevertheless, there is no explicit graph construction in the temporal domain.

B. Graph Convolutional Neural Networks

GCNN extends CNN by consuming data defined on irregular grids. The key challenge is to define convolution over graphs, which is difficult due to the unordered data. According to the definitions of graph convolution, GCNN can be classified into spectral-domain methods and nodal-domain method.

Spectral-domain methods. The convolution over graphs is elegantly defined in the spectral domain, which is the multiplication of the spectral-domain representation of signals. Specifically, the spectral representation is in the graph Fourier transform (GFT) [37] domain, where each signal is projected onto the eigenvectors of the graph Laplacian matrix [37], [38]. The computation complexity, however, is high due to the eigen-decomposition of the graph Laplacian matrix in

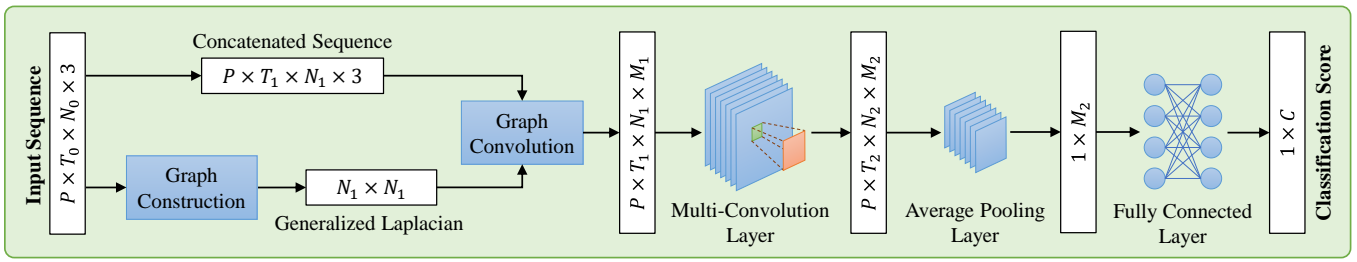


Fig. 2. **The architecture of the proposed GGCN for skeleton-based action recognition.** Our proposed network takes a skeleton sequence as the input, which goes through sequence concatenation and generalized graph construction before feeding into the network. We then employ graph convolution and standard 2D convolution to the concatenated sequence, followed by feature aggregation via average pooling. Thereafter, a fully-connected layer is utilized to generate the output classification scores for C classes.

order to get the eigenvector matrix. Hence, it is improved by [31] through fast localized convolutions, where the Chebyshev expansion is deployed to approximate GFT. Besides, Susnjara et al. introduce the Lancos method for approximation [39]. Spectral GCNN has shown its efficiency in various tasks such as segmentation and classification [30], [40].

Nodal-domain methods. Many techniques are introduced to implement graph convolution directly on each node and its neighbors, i.e., in the nodal domain. Gori et al. introduce recurrent neural networks that operate on graphs in [41]. Duvenaud et al. propose a convolution-like propagation to accumulate local features [29]. Bruna et al. deploy the multi-scale clustering of graphs in convolution to implement multi-scale representation [28]. Furthermore, Niepert et al. define convolution on a sequence of nodes and perform normalization afterwards [42]. Wang et al. propose edge convolution on graphs by incorporating local neighborhood information, which is applied to point cloud segmentation and classification [43]. Nodal-domain methods provide strong localized filters, but it also means it might be difficult to learn the global structure.

III. PRELIMINARIES

We consider an undirected graph $\mathcal{G} = \{\mathcal{V}, \mathcal{E}, \mathbf{A}\}$ composed of a vertex set \mathcal{V} of cardinality $|\mathcal{V}| = n$, an edge set \mathcal{E} connecting vertices, and a weighted *adjacency matrix* \mathbf{A} . \mathbf{A} is a real symmetric $n \times n$ matrix, where $a_{i,j}$ is the weight assigned to the edge (i, j) connecting vertices i and j . We assume non-negative weights, i.e., $a_{i,j} \geq 0$.

The *Laplacian matrix*, defined from the adjacency matrix, can be used to uncover many useful properties of a graph. Among different variants of Laplacian matrices, the *combinatorial graph Laplacian* used in [44], [45] is defined as

$$\mathbf{L} = \mathbf{D} - \mathbf{A}, \quad (1)$$

where \mathbf{D} is the *degree matrix*—a diagonal matrix where $d_{i,i} = \sum_{j=1}^n a_{i,j}$. \mathbf{L} will be leveraged in the proposed variation modeling in Sec. IV-B. The symmetric *normalized Laplacian* is defined as $\mathcal{L} = \mathbf{D}^{-\frac{1}{2}} \mathbf{L} \mathbf{D}^{-\frac{1}{2}}$.

Graph signal refers to data that resides on the vertices of a graph, such as social, transportation, sensor, and neuronal

networks. In our context, we treat each joint in a skeleton sequence as a vertex in a graph, and construct a spatial-temporal graph. Then we define the corresponding graph signal as the coordinates of each joint.

IV. GENERALIZED GRAPH CONVOLUTIONAL NETWORKS

We first overview the architecture of the proposed GGCN. Then we dive into our method starting from modeling of the variation in a skeleton sequence, which leads to the generalized graph construction. Based on this, we discuss generalized graph convolution and feature learning.

A. GGCN architecture

As illustrated in Fig. 2, the input is a skeleton-based action sequence organized as a $P \times T_0 \times N_0 \times 3$ tensor, where P is the number of actors in each sequence, T_0 is the number of frames, N_0 is the number of joints in each frame, and 3 means the dimension of x, y, z coordinates. In order to exploit the spatial-temporal dependencies, we firstly concatenate the input sequence in the unit of 3 consecutive frames, e.g., the $\{1, 2, 3\}^{th}$ frames are concatenated into the first spatial-temporal frame, and the $\{2, 3, 4\}^{th}$ frames into the second one, etc. Thus, the sequence length is changed to T_1 , and the number of joints in each frame is N_1 after frame concatenation, where $T_1 = T_0 - 2$ and $N_1 = N_0 \times 3$. We then construct a generalized graph on each spatial-temporal frame, which will be elaborated in Sec. IV-C, and compute the corresponding symmetric normalized graph Laplacian for describing the connectivities among joints. Secondly, we feed a feature matrix containing the coordinates of skeleton joints in the concatenated sequence and the graph Laplacian into the designed GGCN layer and standard 2D convolution layers for feature extraction. Average pooling is then employed for feature aggregation. Finally, the global feature matrix will go through a fully connected layer followed by a Softmax activation function to output the classification score for C classes. Also, batch normalization is used for all layers before the ReLU activation function.

B. The Modeling of Skeleton's Variation

The fundamental of skeleton-based action recognition is to capture the variation of joints so as to learn motion features for

classification. We propose to model the variation in skeletons via the graph Laplacian defined in Eq. 1.

As discussed in [46], the Laplacian matrix \mathbf{L} is essentially a high-pass operator which captures the variation in the underlying signal. For any signal $\mathbf{x} \in \mathbb{R}^n$, it satisfies

$$(\mathbf{L}\mathbf{x})(i) = \sum_{j \in \mathcal{N}_i} a_{i,j}(x_i - x_j), \quad (2)$$

where $\mathbf{L}\mathbf{x} \in \mathbb{R}^n$, and $(\mathbf{L}\mathbf{x})(i)$ denotes the i -th component of $\mathbf{L}\mathbf{x}$. \mathcal{N}_i is the set of vertices connected to i . This presents that when operating \mathbf{L} on \mathbf{x} , for each vertex, it computes the signal difference among the vertex and its neighboring vertices. In other words, $\mathbf{L}\mathbf{x}$ captures the variation in \mathbf{x} . We thus represent the coordinates of joints in a skeleton sequence as signal defined on a graph, and model its variation via Eq. 2. As will be discussed in Sec. IV-D, a Chebyshev polynomial of $\mathbf{L}\mathbf{x}$ approximates graph convolution in GCNN, thus elegantly enabling learning the variation in a skeleton sequence.

Furthermore, from Eq. 2 we see that the difference among neighboring vertices is weighted by edge weights $a_{i,j}$ in the underlying graph. If the signal difference between vertices i and j is large but the corresponding weight $a_{i,j}$ is rather small or even 0, then this variation will be neglected. On the other hand, if the signal difference is relatively small but $a_{i,j}$ is large, then this variation will be magnified. Hence, the choice of edge weights, i.e., graph construction, plays a crucial role in the variation modeling, which is also the key contribution of our method. We elaborate on the proposed generalized graph construction below.

C. Generalized Graph Construction

The generalized graph construction includes spatial connectivity and temporal connectivity.

Spatial connectivity. For each frame, we model the human body via a connected graph, based on two types of connectivities in particular: strong connections \mathcal{E}_s and weak connections \mathcal{E}_w for describing different correlations. Strong connections aim to capture strong correlations with large weights to emphasize the variation, including physical connectivity and some physical disconnection among joints, while weak connections are used to represent potential correlations among joints that are not physically connected. As shown in Fig. 1, whereas the “head” joint and “hand” joint are not bridged by a bone, we build a weak connectivity between them because of the latent relationship during some actions (e.g., “drink water”). In particular, different weights are assigned to strong and weak edges, i.e., edge weights within a frame are set as

$$a_{i,j} = \begin{cases} w_1, & (i,j) \in \mathcal{E}_s \\ w_2, & (i,j) \in \mathcal{E}_w \\ 0, & \text{otherwise,} \end{cases} \quad (3)$$

where $w_1 > w_2$. We empirically set $w_1 = 5$ and $w_2 = 1$ in our experiments. Note that, while physical connections are intrinsically fixed, it is our freedom to define strong physical disconnections and weak connections. The choice is dependent

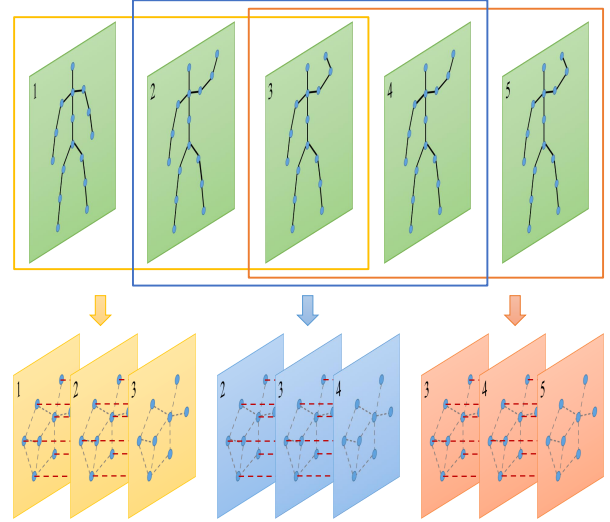


Fig. 3. **Generalized graph construction process.** We construct a generalized graph on each spatial-temporal frame (i.e., every three adjacent frames as a spatial-temporal frame). The yellow, blue, and red groups include three adjacent frames respectively, containing intra-frame connectivities (gray dotted lines) and inter-frame connectivities (red dotted lines).

on the content of skeleton sequences and prior knowledge, which will be discussed in detail in Sec. V-C.

Temporal connectivity. Unlike previous works where each joint is disconnected in the temporal domain or only connected to its corresponding joints in the adjacent frames, we further connect each joint in frame \mathbf{x}_t to the neighborhood of its correspondence in the previous frame \mathbf{x}_{t-1} and subsequent frame \mathbf{x}_{t+1} , which is referred to as *potential edge*, as shown in Fig. 3. This is to capture the latent variation between one joint in frame \mathbf{x}_t and its neighboring joints in the adjacent frames. The receptive field in the temporal domain is thus enlarged by exploiting more neighboring joints, which contributes to learning temporal variation. Taking the action “typing on a keyboard” as an example, the left thumb may have little motion in a short period. However, the left index finger moves relative to the left thumb both spatially and over time, which can be captured by the proposed potential edge. Hence, the final generalized adjacency matrix of consecutive frames $\{\mathbf{x}_{t-1}, \mathbf{x}_t, \mathbf{x}_{t+1}\}$ is defined as

$$\mathbf{A}_g = \begin{bmatrix} \mathbf{A}_{t-1,t-1} & \mathbf{A}_{t-1,t} & \mathbf{O} \\ \mathbf{A}_{t,t-1} & \mathbf{A}_{t,t} & \mathbf{A}_{t,t+1} \\ \mathbf{O} & \mathbf{A}_{t+1,t} & \mathbf{A}_{t+1,t+1} \end{bmatrix}, \quad (4)$$

where $\mathbf{O} \in \mathbb{R}^{n \times n}$ is a zero matrix, $\mathbf{A}_{i,i} \in \mathbb{R}^{n \times n}$ is the weighted adjacency matrix of frame i for representing the intra-frame connectivity, while $\mathbf{A}_{i,j} \in \mathbb{R}^{n \times n}$ ($i \neq j$) is the adjacency matrix between frame i and j for description of the inter-frame connectivity. Based on $\mathbf{A}_g \in \mathbb{R}^{3n \times 3n}$, we compute the graph Laplacian $\mathbf{L} = \mathbf{D} - \mathbf{A}_g$.

D. Generalized Graph Convolution

Following the definition of graph convolution in [31], we adopt the approximation of spectral convolution by Chebyshev

polynomials for efficient implementation:

$$g_\theta * \mathbf{x} \approx \sum_{k=0}^{K-1} \theta_k T_k(\mathcal{L})\mathbf{x}, \quad (5)$$

where $\mathcal{L} = \mathbf{D}^{-\frac{1}{2}}\mathbf{L}\mathbf{D}^{-\frac{1}{2}}$ is the symmetric normalized graph Laplacian as defined in Sec. III, which is employed because the domain of Chebyshev polynomials lies in $[-1, 1]$. θ_k denotes the k -th Chebyshev coefficient and g_θ denotes a convolution kernel. $T_k(\mathcal{L})$ is the Chebyshev polynomial of order k . It is recurrently calculated by $T_k(\mathcal{L}) = 2\mathcal{L}T_{k-1}(\mathcal{L}) - T_{k-2}(\mathcal{L})$, where $T_0(\mathcal{L}) = 1, T_1(\mathcal{L}) = \mathcal{L}$. Hence, the 1st order Chebyshev polynomial computes $\mathcal{L}\mathbf{x}$, which exactly corresponds to Eq. 2, thus capturing the variation in the skeleton data. When $k > 1$, \mathcal{L}^k essentially describes k -hop connectivity, thus incorporating more neighbors and leading to convolution over a larger receptive field.

E. Feature Learning

Having designed the generalized graph convolution, we define the transfer function as follows:

$$\mathbf{y} = \text{ReLU}\left(\sum_{k=0}^{K-1} T_k(\mathcal{L})\mathbf{x}\mathbf{W}_k + \mathbf{b}\right), \quad (6)$$

where $\mathbf{W}_k \in \mathbb{R}^{F_1 \times F_2}$ is a matrix of weight parameters θ'_k as in Eq. 5, which will be learnt from the network, and F_1, F_2 are the dimensions of generated features in two connected layers respectively. $\mathbf{b} \in \mathbb{R}^{n \times F_2}$ is the bias, while ReLU is an activation function.

After the graph convolution layer, we employ standard 2D convolution to the output \mathbf{y} , followed by feature aggregation via average pooling. Thereafter, a fully-connected layer and a Softmax activation function are adopted to generate the output classification scores. We adopt the categorical cross-entropy loss to train the network. The implementation details of our model will be discussed in Sec. V-B.

V. EXPERIMENTS

We evaluate our proposed GGCN on four widely used datasets and compare with state-of-the-art skeleton-based action recognition methods. Experimental details and results are discussed below.

A. Datasets and Evaluation Metrics

NTU RGB+D Dataset [17]: This dataset was captured from 40 human subjects by 3 Microsoft Kinect v2 cameras. It consists of 56880 action sequences with 60 classes. Actions 1-49 were performed by one actor, and actions 50-60 were performed by the other two actors. Each body skeleton was recorded with 25 joints. The benchmark evaluations include Cross-Subject (CS) and Cross-View (CV). In the CS evaluation, 40320 samples from 20 subjects were used for training, and the other samples for testing. In the CV evaluation, samples captured from camera 2 and 3 were used for training, while samples from camera 1 were employed for testing.

Florence 3D Dataset [47]: This dataset contains 215 action sequences of 10 actors with 9 classes. Each body skeleton was collected from Kinect, and recorded with 15 joints. We follow the standard experimental settings to perform leave-one-actor-out validation protocol: we use all the sequences from 9 out of 10 actors for training and the remaining one for testing, and repeat this procedure for all the actors. The resulting 10 classification accuracy values are averaged to get the final accuracy.

UT-Kinect Dataset [10]: This dataset was captured using a single stationary Kinect. It consists of 200 sequences with 10 classes, and each skeleton includes 20 joints. The dataset was recorded by three channels: RGB, depth, and skeleton joint locations, whereas we only use the 3D skeleton joint coordinates. We also adopt the leave-one-actor-out validation protocol to evaluate our model on this dataset.

SYSU 3D Dataset [48]: On this dataset, 40 subjects were asked to perform 12 different activities. Therefore, there are totally 480 action videos on this dataset. For each video, the corresponding RGB frames, depth sequences and skeleton information were captured by a Kinect. We use the sequences performed by 20 subjects for training, and the remaining 20 subjects for testing. We employ the 30-fold cross-subject validation and report the mean accuracy on the dataset.

B. Implementation Details

Our proposed model was implemented with the PyTorch² framework. The number of actors P is set to be 2, 1, 1, 1 for NTU RGB+D, Florence 3D, UT-Kinect, and SYSU 3D dataset respectively. The construction of the generalized graph Laplacian for each dataset will be discussed in detail in Sec. V-C.

Basic Model: Prior to the graph convolution layer, we set a Batch Normalization layer for the batched input data in order to be less careful about data initialization and speed up the training process [49]. In the graph convolution layer, we set the Chebyshev order K to be 4, and the dimension of the weight matrix \mathbf{W}_k in Eq. 6 to be $3n \times 3n$ (i.e., the same as the generalized Laplacian matrix \mathcal{L}). In terms of the standard 2D convolution layer, we set the stride to be 1 and the kernel size to be 9. Each convolution layer follows a Batch Normalization layer. We choose ReLU as the activation function after each convolution layer, and assign the dropout rate 0.5.

Deep Stacking: The above convolutional model can be easily extended into a deep architecture. Taking the above model as one basic layer, we stack it into a multi-layer network architecture, in which the output at the previous layer is used as the input of the next layer. With the increase of layers, the receptive field of convolutional kernels become larger, thus enabling abstracting more global information.

Next, we employ three average pooling layers to pool the P, N , and T dimension respectively, followed by a fully connected layer and a Softmax activation function to output the final classification score. The number of neurons depends

²<https://pytorch.org>

on the output channel of the last convolution layer of the network. We apply Adam [50] optimizer to train the whole model with the initial learning rate 0.1, and decrease it on the 10th epoch. Note that we did not perform any normalization on the skeleton coordinates during data preprocessing.

C. Data Preprocessing

NTU RGB+D Dataset: Due to some missing skeletons in this dataset, we only use the cleaned data³ for action recognition [51]. In order to enhance the robustness of model training, we split the sequences into several segments of equal size in a way similar to [33]. Specifically, we split the whole sequence into 32 segments, and pick the {1, 2, 3, 4}th frame respectively from each segment to generate a large amount of training data.

During the graph construction, according to the characteristics of the actions, we build strong edges across physically connected joints, as well as potentially correlated joint pairs including both *hands*, both *finger tips*, both *thumbs*, both *wrists*, and both *elbows*. Both *hands* and *head* are linked with weak edges.

Florence 3D Dataset: Since the sequences in this dataset contain few frames, we design two ways to generate the training set: sampling and interpolation. For longer sequences (i.e., the length of the sequence is greater than 32), we randomly choose 32 frames; for the other sequences, we calculate the mean of two adjacent frames and insert it into the sequence as a new frame, eventually forming a sequence of 32 frames. For all the sequences, we repeat this operation 3 times to generate the training set.

Regarding the graph construction, we build strong edges for physical connections, as well as both *hands* and *neck*, and both *hands* and *head*. The weak edges are set to be an empty set. Note that we change the weak edges between both *hands* and *head* in the NTU RGB+D dataset to strong edges because they are more closely related in this dataset.

UT-Kinect Dataset: We also adopt sampling and interpolation methods to generate the training set. Here, we set the length of each training sequence to be 64, and repeat the process twice. During the graph construction, we treat physical connections, as well as the connections between both *hands* and *head*, and both *wrists* and *head* as strong edges, while setting weak edges to be an empty set.

SYSU 3D Dataset: Similar to the NTU RGB+D dataset, we split each sequence into 32 segments, and pick the {1, 2, 3, 4, 5}th frame from each segment to generate the training set. However, this dataset does not provide vertex labels, hence we only adopt the adjacency matrix of physical connections provided by the author as the graph within each frame.

Note that, the temporal graph construction is the same on the above datasets, where each joint is not only connected to its corresponding joints in the previous and subsequent frames, but also linked with the neighbors of the corresponding joints.

³<https://github.com/InwoongLee/TS-LSTM>

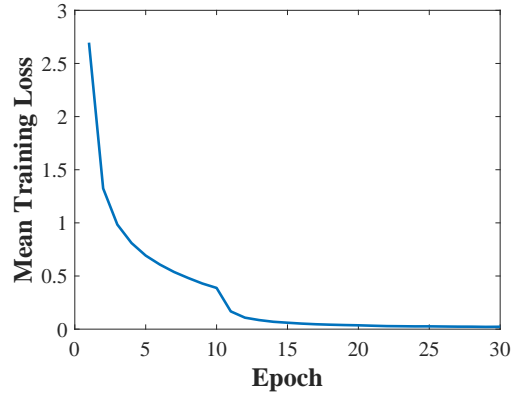


Fig. 4. **GGCN training process on the NTU RGB+D dataset.** This figure demonstrates that, with training, the mean training loss decreases gradually until it converges.

D. Results on NTU RGB+D Dataset

As reported in Tab. I, our model achieves accuracy of 87.5% in CS and 94.3% in CV respectively. Also, as will be discussed in the ablation study, the proposed intra-connections improve the performance by 0.7% in CS and 1.4% in CV over the baseline method (*GGCN+Bone*), while the proposed temporal connectivities lead to 3.2% gain in CS and 3.1% gain in CV, validating the effectiveness of our method.

Comparison with the State-of-the-arts: We present the comparison with the state-of-the-art methods in Tab. I. We see that our method outperforms all the other state-of-the-art methods. Specifically, compared with the latest state-of-the-art method SR-TSL [52], our model leads to 2.7% gain in CS and 1.9% gain in CV respectively, which demonstrates the superiority of our method.

Ablation Study: In order to validate the advantages of the proposed generalized graph construction in our method, we evaluate various graph construction methods progressively and design the following incomplete models. Model 1 is *GGCN + Bone*, in which only joints connected with a bone are linked with graph edges. This kind of graph construction is commonly used in existing graph-based skeleton recognition [32], [33], [34], and thus is the baseline. Model 2 is *GGCN + Bone + Intra-connection* (non-physical), where connectivities are further added to joints that are not physically connected within each frame, including strong and weak edges for capturing latent dependencies. This kind of connectivities are previously exploited in [34]. Model 3 is our complete model with extra temporal connections included. We observe that Model 1 already achieves competitive performance with the state-of-the-art methods, which shows the effectiveness of the proposed GGCN. With additional intra-connectivities, Model 2 improves the accuracy by 0.7% in CS and 1.4% in CV over Model 1, validating the benefits of non-physical connections. Further, when the temporal connections are exploited, the complete model achieves 2.5% gain in CS and 1.7% gain in CV over Model 2. We thus conclude that both

TABLE I
COMPARISONS ON THE NTU RGB+D DATASET (%).

Methods	CS	CV	Year
Dynamic Skeletons [48]	60.2	65.2	2015
Part-aware LSTM [17]	62.9	70.3	2016
Geometric Features [20]	70.3	82.4	2017
LSTM-CNN [21]	82.9	91.0	2017
Two-Stream CNN [24]	83.2	89.3	2017
ST-LSTM (Tree)+Trust Gate [23]	69.2	77.7	2018
Deep STGC _K [33]	74.9	86.3	2018
ST-GCN [32]	81.5	88.3	2018
DPRL [34]	83.5	89.8	2018
SR-TSL [52]	84.8	92.4	2018
GGCN + Bone	84.3	91.2	
GGCN + Bone + Intra-connection	85.0	92.6	
Complete GGCN model	87.5	94.3	

the proposed non-physical intra-connectivities and the explicit temporal connections make contributions to skeleton-based action recognition, in which the temporal connectivities are more crucial.

Analysis of the Training Process: Moreover, Fig. 4 shows the training process of our model on the NTU RGB+D dataset in CS validation. The horizontal axis is the index of the training epoch, while the vertical axis refers to the mean training loss. We observe that the mean training loss decreases rapidly in the first 10 epochs due to the large learning rate. We update the learning rate at the 10th epoch, after which the mean training loss decreases slowly. Until the 20th epoch, the mean training loss basically converges, validating the effectiveness of our model.

E. Results on SYSU 3D Dataset

We compare our method with the state-of-the-art skeleton-based action recognition methods on SYSU 3D Dataset, which are presented in Tab. II. Our proposed method outperforms all the other state-of-the-art methods on this dataset, achieving accuracy improvement of 1.0% over the previous best method DPRL [34].

Note that, as vertex labels are not provided by this dataset, we can only build strong physical connections from the given adjacency matrix within each frame while abandoning weak edges. Hence, we provide ablation study with Model 1 (*GGCN + Bone*) in Tab. II. We see that our complete model achieves 2.7% improvement over the baseline method. This validates the benefits of incorporating explicit temporal connectivities across consecutive frames again.

Also, the confusion matrix of our result is demonstrated in Fig. 5. We see that the matrix is diagonally dominant on all the 12 classes, which validates that our method achieves excellent classification results on this dataset. Besides, we note that our model sometimes confuses the activity of “mopping” with “sweeping”, which is mainly due to the highly similar motions in the two actions.

F. Results on UT-Kinect Dataset

As listed in Tab. III, our method achieves comparable accuracy of 98.5% to [34], and outperforms all the other

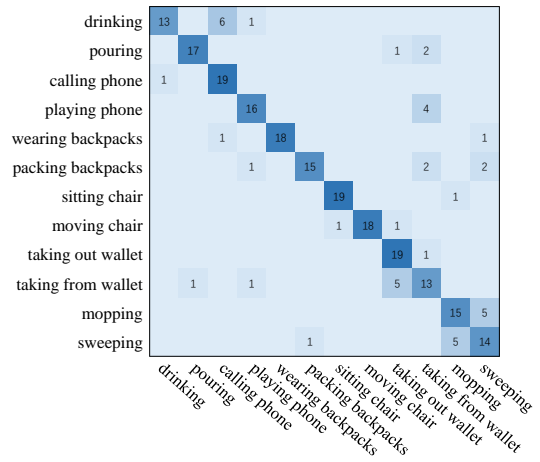


Fig. 5. Confusion matrix of GGCN on SYSU 3D dataset.

TABLE II
COMPARISONS ON THE SYSU 3D DATASET (%).

Methods	Accuracy	Year
Dynamic Skeletons [48]	75.5	2015
LAFF (SKL) [53]	54.2	2016
ST-LSTM (Tree) [23]	73.4	2018
ST-LSTM (Tree) + Trust Gate [23]	76.5	2018
DPRL [34]	76.9	2018
GGCN + Bone	75.2	
Complete GGCN model	77.9	

methods. Note that the performance difference among all the methods is rather small in general. The reason is that this dataset includes several very similar actions, which are difficult to distinguish without RGB or depth data.

Also, we perform the same ablation study as in Sec. V-D, as reported in Tab. III. We observe that Model 2 improves the accuracy by 0.5% over Model 1 with additional intra-connectivities. Further, when the temporal connectivities are built, the complete model achieves 1.1% improvement over Model 2, which demonstrates the advantages of the proposed generalized graph construction.

G. Results on Florence 3D Dataset

We present the performance comparison with the state-of-the-art methods on the Florence 3D dataset in Tab. IV. Our

TABLE III
COMPARISONS ON THE UT-KINECT DATASET (%).

Methods	Accuracy	Year
Lie Group [14]	97.1	2014
LARP+mfPCA [54]	94.9	2015
SPGK [13]	97.4	2016
ST-NBNN [16]	98.0	2017
Bi-LSTM [22]	96.9	2018
ST-LSTM(Tree) + Trust Gate [23]	97.0	2018
DPRL [34]	98.5	2018
GGCN + Bone	96.9	
GGCN + Bone + Intra-connection	97.4	
Complete GGCN model	98.5	

TABLE IV
COMPARISONS ON THE FLORENCE 3D DATASET (%).

Methods	Accuracy	Year
Lie Group [14]	90.9	2014
LARP+mfPCA [54]	89.7	2015
Rolling Rotations [55]	91.4	2016
SPGK [13]	91.6	2016
Transion Forests [56]	94.2	2017
MIMTL [57]	95.3	2017
Bi-LSTM [22]	93.0	2018
Deep STGC _K [33]	99.1	2018
GGCN + Bone	95.5	
GGCN + Bone + Intra-connection	95.6	
Complete GGCN model	98.4	

method achieves classification accuracy of 98.5%, outperforming all the other state-of-the-art methods significantly except Deep STGC_K [33]. The reason is that Deep STGC_K benefits from the design philosophy of autoregressive moving average model, which is tailored for time sequences. Due to the few joints in each frame and few frames in the sequence, our model is difficult to capture subtle variation from few joints. Thus we misclassify “drink from a bottle” and “answer phone”, “read watch” and “clap”, which is difficult to distinguish even with human vision.

Moreover, Tab. IV reports the results of ablation study. We achieve 0.1% improvement from non-physical intra-connections compared with GGCN + Bone, and another 2.8% improvement from temporal connections compared with GGCN + Bone + Intra-connection. This validates the effectiveness of the proposed graph construction, in which the temporal connectivities are vital.

VI. CONCLUSION

We propose a generalized graph convolutional network (GGCN) for skeleton-based action recognition, aiming to fully exploit both spatial and temporal dependencies among human joints via generalized graph construction. The proposed generalized graph not only captures intrinsic physical connections, but also models strong and weak non-physical connectivities over consecutive frames so as to represent latent correlations for better recognition. We then employ spectral graph convolution with high-order Chebyshev approximation for feature extraction. Extensive experiments demonstrate the superiority of our method.

REFERENCES

- [1] Karen Simonyan and Andrew Zisserman. Two-stream convolutional networks for action recognition in videos. In *Advances in Neural Information Processing Systems (NIPS)*, pages 568–576, 2014. 1
- [2] Du Tran, Lubomir Bourdev, Rob Fergus, Lorenzo Torresani, and Manohar Paluri. Learning spatiotemporal features with 3d convolutional networks. In *IEEE International Conference on Computer Vision (CVPR)*, pages 4489–4497, 2015. 1
- [3] Limin Wang, Yu Qiao, and Xiaoou Tang. Action recognition with trajectory-pooled deep-convolutional descriptors. In *IEEE conference on Computer Vision and Pattern Recognition (CVPR)*, pages 4305–4314, 2015. 1
- [4] Limin Wang, Yuanjun Xiong, Zhe Wang, Yu Qiao, Dahua Lin, Xiaoou Tang, and Luc Van Gool. Temporal segment networks: Towards good practices for deep action recognition. In *European Conference on Computer Vision (ECCV)*, pages 20–36, 2016. 1
- [5] Yue Zhao, Yuanjun Xiong, Limin Wang, Zhirong Wu, Xiaoou Tang, and Dahua Lin. Temporal action detection with structured segment networks. *IEEE International Conference on Computer Vision (ICCV)*, 2, 2017. 1
- [6] Yong Du, Wei Wang, and Liang Wang. Hierarchical recurrent neural network for skeleton based action recognition. In *IEEE Conference on Computer Vision and Pattern Recognition (CVPR)*, pages 1110–1118, 2015. 1, 2
- [7] Jun Liu, Amir Shahroudy, Dong Xu, and Gang Wang. Spatio-temporal lstm with trust gates for 3d human action recognition. In *European Conference on Computer Vision (ECCV)*, pages 816–833, 2016. 1, 2
- [8] Jamie Shotton, Andrew Fitzgibbon, Mat Cook, Toby Sharp, Mark Finocchio, Richard Moore, Alex Kipman, and Andrew Blake. Real-time human pose recognition in parts from single depth images. In *IEEE Conference on Computer Vision and Pattern Recognition (CVPR)*, pages 1297–1304, 2011. 1
- [9] Fei Han, Brian Reily, William Hoff, and Hao Zhang. Space-time representation of people based on 3d skeletal data: A review. *Computer Vision and Image Understanding (CVIU)*, 158:85–105, 2017. 1
- [10] Lu Xia, Chia-Chih Chen, and Jake K Aggarwal. View invariant human action recognition using histograms of 3d joints. *IEEE Conference on Computer vision and pattern recognition workshops (CVPRW)*, pages 20–27, 2012. 1, 5
- [11] Jiang Wang, Zicheng Liu, Ying Wu, and Junsong Yuan. Mining actionlet ensemble for action recognition with depth cameras. In *IEEE Conference on Computer Vision and Pattern Recognition (CVPR)*, pages 1290–1297, 2012. 1
- [12] Mohammad Abdelaziz Gowayyed, Marwan Torki, Mohamed Elsayed Hussein, and Motaz El-Saban. Histogram of oriented displacements (hod): Describing trajectories of human joints for action recognition. In *International Joint Conference on Artificial Intelligence (IJCAI)*, volume 13, pages 1351–1357, 2013. 1
- [13] Pei Wang, Chunfeng Yuan, Weiming Hu, Bing Li, and Yanning Zhang. Graph based skeleton motion representation and similarity measurement for action recognition. In *European Conference on Computer Vision (ECCV)*, pages 370–385, 2016. 1, 7, 8
- [14] Raviteja Vemulapalli, Felipe Arrate, and Rama Chellappa. Human action recognition by representing 3d skeletons as points in a lie group. In *IEEE Conference on Computer Vision and Pattern Recognition (CVPR)*, pages 588–595, 2014. 1, 2, 7, 8
- [15] Chunyu Wang, Yizhou Wang, and Alan L Yuille. Mining 3d key-pose-motifs for action recognition. In *IEEE Conference on Computer Vision and Pattern Recognition (CVPR)*, pages 2639–2647, 2016. 1
- [16] Junwu Weng, Chaoqun Weng, and Junsong Yuan. Spatio-temporal naive-bayes nearest-neighbor (st-nbnn) for skeleton-based action recognition. In *IEEE Conference on Computer Vision and Pattern Recognition (CVPR)*, pages 4171–4180, 2017. 1, 2, 7
- [17] Amir Shahroudy, Jun Liu, Tian-Tsong Ng, and Gang Wang. Ntu rgb+d: A large scale dataset for 3d human activity analysis. *IEEE Conference on Computer Vision and Pattern Recognition (CVPR)*, pages 1010–1019, 2016. 1, 2, 5, 7
- [18] Wentao Zhu, Cuiling Lan, Junliang Xing, Wenjun Zeng, Yanghao Li, Li Shen, and Xiaohui Xie. Co-occurrence feature learning for skeleton based action recognition using regularized deep lstm networks. In *AAAI Conference on Artificial Intelligence (AAAI)*, volume 2, page 6, 2016. 1, 2
- [19] Sijie Song, Cuiling Lan, Junliang Xing, Wenjun Zeng, and Jiaying Liu. An end-to-end spatio-temporal attention model for human action recognition from skeleton data. In *AAAI Conference on Artificial Intelligence (AAAI)*, volume 1, pages 4263–4270, 2017. 1, 2
- [20] Songyang Zhang, Xiaoming Liu, and Jun Xiao. On geometric features for skeleton-based action recognition using multilayer lstm networks. In *IEEE Winter Conference on Applications of Computer Vision (WACV)*, pages 148–157, 2017. 1, 2, 7
- [21] Chuankun Li, Pichao Wang, Shuang Wang, Yonghong Hou, and Wanqing Li. Skeleton-based action recognition using lstm and cnn. In *International Conference on Multimedia & Expo Workshops (ICMEW)*, pages 585 – 590, July 2017. 1, 2, 7
- [22] Amor Ben Tanfous, Hassen Drira, and Boulbaba Ben Amor. Coding kendall’s shape trajectories for 3d action recognition. *IEEE Computer Vision and Pattern Recognition (CVPR)*, 2018. 1, 2, 7, 8
- [23] Jun Liu, Amir Shahroudy, Dong Xu, Alex C Kot, and Gang Wang. Skeleton-based action recognition using spatio-temporal lstm network with trust gates. In *IEEE Transactions on Pattern Analysis and Machine Intelligence (TPAMI)*, volume 40, pages 3007 – 3021, 2018. 1, 2, 7

- [24] Chao Li, Qiaoyong Zhong, Di Xie, and Shiliang Pu. Skeleton-based action recognition with convolutional neural networks. *IEEE International Conference on Multimedia & Expo Workshops (ICMEW)*, July 2017. 1, 2, 7
- [25] Qihong Ke, Mohammed Bennamoun, Senjian An, Ferdous Sohel, and Farid Boussaid. A new representation of skeleton sequences for 3d action recognition. In *IEEE Conference on Computer Vision and Pattern Recognition (CVPR)*, pages 4570–4579, 2017. 1, 2
- [26] Tae Soo Kim and Austin Reiter. Interpretable 3d human action analysis with temporal convolutional networks. In *IEEE Conference on Computer Vision and Pattern Recognition Workshops (CVPRW)*, pages 1623–1631, 2017. 1, 2
- [27] Mengyuan Liu, Hong Liu, and Chen Chen. Enhanced skeleton visualization for view invariant human action recognition. *Pattern Recognition (PR)*, 68:346–362, 2017. 1, 2
- [28] Joan Bruna, Wojciech Zaremba, Arthur Szlam, and Yann LeCun. Spectral networks and locally connected networks on graphs. *Computer Science*, 2013. 1, 3
- [29] David K Duvenaud, Dougal Maclaurin, Jorge Iparraguirre, Rafael Bombarell, Timothy Hirzel, Alán Aspuru-Guzik, and Ryan P Adams. Convolutional networks on graphs for learning molecular fingerprints. In *Advances in Neural Information Processing Systems (NIPS)*, pages 2224–2232, 2015. 1, 3
- [30] Thomas N Kipf and Max Welling. Semi-supervised classification with graph convolutional networks. *arXiv preprint arXiv:1609.02907*, 2016. 1, 3
- [31] Michaël Defferrard, Xavier Bresson, and Pierre Vandergheynst. Convolutional neural networks on graphs with fast localized spectral filtering. In *Advances in Neural Information Processing Systems (NIPS)*, pages 3844–3852, 2016. 1, 2, 3, 4
- [32] Sijie Yan, Yuanjun Xiong, and Dahua Lin. Spatial temporal graph convolutional networks for skeleton-based action recognition. *AAAI Conference on Artificial Intelligence (AAAI)*, 2018. 1, 2, 6, 7
- [33] Chaolong Li, Zhen Cui, Wenming Zheng, Chunyan Xu, and Jian Yang. Spatio-temporal graph convolution for skeleton based action recognition. *AAAI Conference on Artificial Intelligence (AAAI)*, 2018. 1, 2, 6, 7, 8
- [34] Yansong Tang, Yi Tian, Jiwen Lu, Peiyang Li, and Jie Zhou. Deep progressive reinforcement learning for skeleton-based action recognition. In *IEEE Conference on Computer Vision and Pattern Recognition (CVPR)*, pages 5323–5332, 2018. 1, 2, 6, 7
- [35] Fan RK Chung. *Spectral graph theory*. Number 92. American Mathematical Soc., 1997. 2
- [36] Mohamed E Hussein, Marwan Torki, Mohammad Abdelaziz Gowayed, and Motaz El-Saban. Human action recognition using a temporal hierarchy of covariance descriptors on 3d joint locations. In *International Joint Conference on Artificial Intelligence (IJCAI)*, volume 13, pages 2466–2472, 2013. 2
- [37] David K Hammond, Pierre Vandergheynst, and Rémi Gribonval. Wavelets on graphs via spectral graph theory. *Applied and Computational Harmonic Analysis (ACHA)*, 30(2):129–150, 2011. 2
- [38] Mikael Henaff, Joan Bruna, and Yann LeCun. Deep convolutional networks on graph-structured data. *arXiv preprint arXiv:1506.05163*, 2015. 2
- [39] Ana Susnjara, Nathanael Perraudin, Daniel Kressner, and Pierre Vandergheynst. Accelerated filtering on graphs using lanczos method. *arXiv preprint arXiv:1509.04537*, 2015. 3
- [40] Gusi Te, Wei Hu, Zongming Guo, and Amin Zheng. Rgcnn: Regularized graph cnn for point cloud segmentation. In *ACM Multimedia Conference (MM)*, October 2018. 3
- [41] Marco Gori, Gabriele Monfardini, and Franco Scarselli. A new model for learning in graph domains. In *IEEE International Joint Conference on Neural Networks (IJCNN)*, volume 2, pages 729–734, 2005. 3
- [42] Mathias Niepert, Mohamed Ahmed, and Konstantin Kutzkov. Learning convolutional neural networks for graphs. In *International Conference on Machine Learning (ICML)*, pages 2014–2023, 2016. 3
- [43] Yue Wang, Yongbin Sun, Ziwei Liu, Sanjay E Sarma, Michael M Bronstein, and Justin M Solomon. Dynamic graph cnn for learning on point clouds. *arXiv preprint arXiv:1801.07829*, 2018. 3
- [44] Godwin Shen, W-S Kim, Sunil K Narang, Antonio Ortega, Jaejoon Lee, and Hocheon Wey. Edge-adaptive transforms for efficient depth map coding. In *Picture Coding Symposium (PCS)*, pages 566–569, 2010. 3
- [45] Wei Hu, Gene Cheung, Antonio Ortega, and Oscar C Au. Multiresolution graph fourier transform for compression of piecewise smooth images. *IEEE Transactions on Image Processing (TIP)*, 24(1):419–433, 2015. 3
- [46] David I Shuman, Sunil K. Narang, Pascal Frossard, Antonio Ortega, and Pierre Vandergheynst. The emerging field of signal processing on graphs: Extending high-dimensional data analysis to networks and other irregular domains. *IEEE Signal Processing Magazine*, 30:83–98, 2013. 4
- [47] Lorenzo Seidenari, Vincenzo Varano, Stefano Berretti, Alberto Bimbo, and Pietro Pala. Recognizing actions from depth cameras as weakly aligned multi-part bag-of-poses. *IEEE Conference on Computer Vision and Pattern Recognition Workshops (CVPRW)*, pages 479–485, 2013. 5
- [48] Jian-Fang Hu, Wei-Shi Zheng, Jianhuang Lai, and Jianguo Zhang. Jointly learning heterogeneous features for rgb-d activity recognition. *IEEE Conference on Computer Vision and Pattern Recognition (CVPR)*, pages 5344–5352, 2015. 5, 7
- [49] Sergey Ioffe and Christian Szegedy. Batch normalization: Accelerating deep network training by reducing internal covariate shift. In *International Conference on International Conference on Machine Learning (ICML)*, volume 37, pages 448 – 456, July 2015. 5
- [50] Diederik P Kingma and Jimmy Ba. Adam: A method for stochastic optimization. *Computer Science*, 2014. 6
- [51] Inwoong Lee, Doyoung Kim, Seoungyoon Kang, and Sanghoon Lee. Ensemble deep learning for skeleton-based action recognition using temporal sliding lstm networks. *IEEE International Conference on Computer Vision (ICCV)*, pages 1012–1020, 2017. 6
- [52] Chenyang Si, Ya Jing, Wei Wang, Liang Wang, and Tieniu Tan. Skeleton-based action recognition with spatial reasoning and temporal stack learning. *European Conference on Computer Vision (ECCV)*, pages 106–121, 2018. 6, 7
- [53] Jian-Fang Hu, Wei-Shi Zheng, Lianyang Ma, Gang Wang, and Jianhuang Lai. Real-time rgb-d activity prediction by soft regression. In *European Conference on Computer Vision (ECCV)*, pages 280–296, 2016. 7
- [54] Rushil Anirudh, Pavan Turaga, Jingyong Su, and Anuj Srivastava. Elastic functional coding of human actions: From vector-fields to latent variables. In *IEEE Conference on Computer Vision and Pattern Recognition (CVPR)*, pages 3147–3155, 2015. 7, 8
- [55] Raviteja Vemulapalli and Rama Chellapa. Rolling rotations for recognizing human actions from 3d skeletal data. In *IEEE Conference on Computer Vision and Pattern Recognition (CVPR)*, pages 4471–4479, 2016. 8
- [56] Guillermo Garcia-Hernando and Tae-Kyun Kim. Transition forests: Learning discriminative temporal transitions for action recognition and detection. In *IEEE Conference on Computer Vision and Pattern Recognition (CVPR)*, pages 432–440, 2017. 8
- [57] Yanhua Yang, Cheng Deng, Shangqian Gao, Wei Liu, Dapeng Tao, and Xinbo Gao. Discriminative multi-instance multitask learning for 3d action recognition. *IEEE Transactions on Multimedia (TMM)*, 19(3):519–529, 2017. 8